Engineering Notes

Trajectory Optimization for Multitarget Tracking Using Joint Probabilistic Data Association Filter

Shaoming He,* Hyo-Sang Shin,† and Antonios Tsourdos‡
*Cranfield University, Cranfield, England MK43 0AL,
United Kingdom*

https://doi.org/10.2514/1.G004249

I. Introduction

AIRBORNE target tracking is a key enabling technology in many civilian and military applications, including situation awareness [1–3], vehicle monitoring [4,5], public surveillance [6], and traffic management [7]. However, reliable target tracking becomes challenging when dealing with highly complex multitarget tracking (MTT) problem. The objective of MTT is to simultaneously estimate the number of targets and their states. In MTT, except for the fact that the number of targets varies randomly in time, the received measurements are also subject to a certain degree of uncertainties: unknown source origin, miss detections, and false alarms. There are several elegant solutions available in the literature to address the measurement uncertainty problem in MTT: nearest neighbor (NN) filter [8], probabilistic data association (PDA) filter [9], joint probabilistic data association (JPDA) filter [10,11], and multiple hypothesis tracking (MHT) [12–14]. This Note adapts the JPDA filter as the baseline multitarget tracker because of its balance between estimation accuracy and computational cost.

It is known that the estimation accuracy depends not only on the filter performance but also on the relative geometry between the unmanned aerial vehicle (UAV) and the targets [15–17]. For this reason, trajectory optimization or path planning that directly or indirectly minimizes the estimation error has been widely studied in the literature. Optimal UAV trajectories that minimize the estimation error are generated in [18–21] using numerical optimizations by maximizing the determinant of Fisher information matrix (FIM) over a finite time horizon. The rationale of using FIM for a cost function lies in that the inverse of FIM prescribes a lower bound, also known as posterior Cramer–Rao bound (PCRB), of the estimation error covariance of an unbiased filter [22]. By maximizing the approximate lower bound of FIM, an optimal variable deviated pursuit guidance algorithm that improves the cooperative estimation performance was proposed in [23] for a UAV rendezvous mission. Several trajectory optimization algorithms for

spacecraft rendezvous were reported in [24–26] to improve the estimation quality. An algorithm for active localization of stationary targets using ground robots was suggested in [27,28] by leveraging the trace of error covariance matrix as the cost function.

Although the aforementioned algorithms can bring significant benefits in target tracking, they are mainly limited to single target tracking (STT) scenarios. The aim of this Note is, therefore, to propose a new optimization framework for a fixed-wing UAV to find its optimal trajectory that improves the MTT estimation performance. In trajectory optimization, it is known that formulating a suitable cost function, or objective function, is of significant importance. The difficulty in formulating a simple yet pertinent cost function for MTT, however, naturally arises in the inevitable data association uncertainty and the random number of targets. To simplify the problem formulation, the authors in [4,29,30] leveraged the FIM, analogous to the approach used in STT, to formulate the cost function in trajectory optimization for MTT: the objective function is defined as the summation of all FIMs from all existing targets. This simple cost function, however, ignores the inherent data association uncertainty in MTT and thus cannot really reflect the estimation performance of the tracker. Instead of using FIM, the Rényi information divergence between the posterior and prior distributions was used in [31] for sensor scheduling to track multiple targets. However, calculating the information-theoretic Rényi information divergence for a Gaussian mixture requires computationally expensive Monte-Carlo techniques. The authors in [32] derived the MTT PCRB by taking into account data association uncertainty. Although this performance metric could be an ideal candidate objective function in trajectory optimization for MTT, calculating the MTT PCRB requires computationally expensive Monte-Carlo integration. Therefore, these optimization frameworks might not be suitable for online implementation.

Unlike STT, the objective of an MTT algorithm is to simultaneously estimate the number of targets and their states. The cost function, therefore, should be a balance between cardinality estimation performance and target localization performance. Taking this factor into account, this Note formulates an analytical cost function for MTT by leveraging the properties of the JPDA filter. The cost function developed is a weighted sum of multitarget estimation variance and cardinality estimation variance. By minimizing the cost function, we can therefore increase the confidence level of JPDA filter, thus indirectly improving the estimation performance. As discussed later, the multitarget estimation variance can also be viewed as the data association uncertainty. This means that the proposed cost function also provides the possibility to improve the quality of data association. Incorporating the objective function formulated with physical constraints, for example, turning rate limit, a constrained trajectory optimization framework for MTT is proposed. Because the objective function is nonconvex in general, an approximate solution is obtained by the control input discretization. The resultant solution, given as heading angle input command, is simple to be implemented in practice through an onboard heading tracking control system.

Realistic scenarios are simulated to illustrate and evaluate the performance of the proposed algorithm, and the results clearly demonstrate that the proposed approach can significantly improve the MTT estimation performance, especially when the detection probability is time varying.

The rest of the Note is organized as follows. Section II presents some mathematical models used in this study. Section III gives a brief review of JPDA filter, and Sec. IV provides the details of the proposed cost function, followed by the trajectory optimization solution shown in Sec. V. Finally, some numerical simulations are demonstrated.

II. Mathematical Models

This section provides necessary preliminaries of several important mathematical models to facilitate the analysis in the following sections.

A. UAV Kinematics Model

This work assumes that the UAV is equipped with a high-performance low-level flight control system that provides roll, pitch, and yaw stability as well as velocity tracking, heading, and altitude hold functions. This study aims to design guidance input, for example, heading angle command, and feed this to the low-level controller for multiple targets localization and is constrained to the two-dimensional (2-D) motions. The UAV's kinematics in a 2-D environment is given by

$$
\begin{aligned}
\dot{p}_x^u &= V_u \cos \psi_u \\
\dot{p}_y^u &= V_u \sin \psi_u
\end{aligned}
\tag{1}
$$

where (p_x^u, p_y^u) stands for the UAV position in an inertial coordinate. ψ_u is the UAV heading angle, and V_u denotes the UAV speed. For simplicity, the following general assumption is made.

Assumption 1: The speed of UAV is assumed to be constant. Note that the UAV speed is often predefined for operational reasons, for example, endurance and mission objectives.

In practice, the heading change of a fixed-wing UAV between two consecutive time steps is constrained due to physical turning rate limitation as

$$
|\psi_{u,k} - \psi_{u,k-1}| \leq \psi_{\max} \triangleq \dot{\psi}_{\max} T_s
\tag{2}
$$

where $\psi_{u,k}$ represents the heading angle at time step k, $\dot{\psi}_{\max}$ the maximum permissible turning rate of the UAV, and T_s the sampling time.

B. Multitarget State and Measurement Model

Suppose that there are N_k targets and M_k sensor measurements at scan k. A multitarget state X_k and a multitarget measurement Z_k are then defined as

$$
X_k = \{x_k^1, \ldots, x_k^{N_k}\} \quad Z_k = \{z_k^0, z_k^1, \ldots, z_k^{M_k}\}
\tag{3}
$$

where x_k^i denotes the ith target at scan k, $z_k^j (j \neq 0)$ the jth measurement received at scan k, and z_k^0 the dummy measurement for convenient representation of miss detection.

Consider the following dynamical system of target:

$$
\begin{aligned}
x_k^i &= f_{k-1}^i(x_{k-1}^i) + w_{k-1}^i \\
z_k^i &= h_k^i(x_k^i) + v_k^i
\end{aligned}
\tag{4}
$$

where $x_k^i \in \mathbb{R}^n$ and $z_k^i \in \mathbb{R}^m$ denote the system state and the corresponding measurement of the ith target at time step k. The nonlinear functions $f_k^i(x_k^i)$ and $h_k^i(x_k^i)$ correspond to the system state evolution and measurement equations, respectively. The signals w_k^i and v_k^i are process noise and measurement noise, which are assumed to be zero-mean Gaussian with covariances Q_k^i and R_k^i. For convenience, we make the following general assumptions, which are widely accepted in MTT problems.

Assumption 2: Each target can generate at most one measurement, and each measurement can originate from at most one target. Each target-generated measurement is independent of each other and is detected with probability P_D. Notice that the detection probability, by default, depends on the relative geometry between the UAV and the target and therefore is usually a time-varying variable.

Assumption 3: The clutter distribution is assumed to be unknown a priori and is thus considered as Poisson distribution. Clutters or false alarms are modeled by a local Poisson point process with intensity $\lambda_{\mathrm{FA}} = N_{\mathrm{FA}}/V_s$, with N_{FA} being the average number of false alarms received at each scan and V_s being the sensor volume.

C. Target Existence Model

In MTT, there is no prior information on the source of received measurements. That is, each measurement may be spurious, for example, false alarm, or from one existing/new target. For this reason, both true tracks, representing real targets, and false tracks are generated and updated. The number of targets at time instant k is also a random variable in an MTT problem: one target might suddenly disappear or appear in the sensor's field of view. Because of these facts, a track confirmation and deletion logic is essential in MTT to confirm the majority of true tracks and terminates most false tracks.

In this Note, each track is confirmed or terminated using thresholding based on target existence probability $\rho_k^i \triangleq p(\chi_k^i | Z_k)$, with χ_k^i being the event of existence of the ith target at scan k. If ρ_k^i is larger than a upper threshold α_1, then the ith track is confirmed; once ρ_k^i is below a certain lower bound α_2, the ith track is immediately deleted. For the case where $\alpha_2 \leq \rho_k^i \leq \alpha_1$, the ith track is tentative and requires more information to confirm or delete. The time evolution of χ_k^i can be formulated by

$$
p(\chi_k^i | Z_{k-1}) = P_S p(\chi_{k-1}^i | Z_{k-1})
\tag{5}
$$

where P_S denotes the surviving probability. For target birth, the following general assumption is used in this Note.

Assumption 4: The number of new targets is assumed to be unknown a priori and is thus considered as Poisson distribution. New targets are modeled by a local Poisson point process with intensity $\lambda_B = N_B/V_s$, with N_B being the average number of new targets.

Remark 1: Note that an MTT algorithm creates a new track for each measurement received at every scan. This means that the number of tracks grows exponentially as time goes. To maintain computational feasibility, we use a thresholding-based track deletion logic to remove unreliable tracks. Therefore, the tracks kept at each scan include confirmed tracks and tentative tracks.

III. Joint Probabilistic Data Association Filter

In a general MTT mission, the relationship between targets and measurements is unknown and the number of targets is also a random variable. The challenge is that each target can appear and disappear at any place and any time. Data association is a widely accepted and plausible solution to resolve the problem of measurement origin uncertainty. This technique discerns target-generated measurements from clutters and finds the mappings between targets and measurements, and therefore is the key in MTT.

JPDA is a well-established single-scan data association approach based on probabilistic reasoning [10,11]. This approach associates the measurements to the targets under the assumption that the relationship between targets and measurements satisfies: 1) each measurement (except for the dummy one) is assigned to at most one target, and 2) each target is uniquely assigned to a measurement. Based on the assumption, the approach uses the joint association hypothesis that is denoted as $\Theta_k = \{\theta_k^i\}$, $i \in \{1, 2, \ldots, N_{k|k-1} + M_k\}$. The joint association hypothesis and corresponding probability measures play a key role in the data association filter. For each pre-existed target $i \in \{1, 2, \ldots, N_{k|k-1}\}$, define $\theta_k^i \in \{0, 1, \ldots, M_k\}$ as the association hypothesis, where $N_{k|k-1}$ stands for the predicted number of targets at scan k. As we have no information on target birth/death at scan k before receiving the measurements, $N_{k|k-1}$ is determined as $N_{k|k-1} = N_{k-1|k-1}$. The single association event $\theta_k^i = j$ refers to the fact that the jth measurement originates from the ith target and $\theta_k^i = 0$ represents miss detection. We create a new track for each measurement $j \in \{1, 2, \ldots, M_k\}$ at scan k, and the association event for these new targets are defined by $\theta_k^{N_{k|k-1}+j} \in \{N_{k|k-1} + 1, \ldots, N_{k|k-1} + M_k\}$. That is, if target $N_{k|k-1} + j$ is associated with the jth measurement, then $\theta_k^{N_{k|k-1}+j} = N_{k|k-1} + j$. Under the assumption that each single association event is independent, the minimum-mean-squared-error (MMSE) estimate of each target is given by

$$p(x_k^i|\chi_k^i, Z_k) = \sum_{\theta_k^i} p(x_k^i|\theta_k^i, \chi_k^i, Z_k)p(\theta_k^i|\chi_k^i, Z_k) \qquad (6)$$

In practice, propagation of mixture is computationally intractable due to the explosion of mixture terms. JPDA approximates mixture (6) by a single probability density function based on simple moment-preserving approach. More specifically, the state correction $x_{k|k}^i$ of the ith target and its corresponding covariance $P_{k|k}^i$ are obtained as

$$x_{k|k}^i = \sum_{j=0}^{M_k} \beta_j^i x_{k|k}^{i,j}$$

$$P_{k|k}^i = \sum_{j=0}^{M_k} \beta_j^i \{P_{k|k}^{i,j} + (x_{k|k}^{i,j} - x_{k|k}^i)(x_{k|k}^{i,j} - x_{k|k}^i)^T\} \qquad (7)$$

where $x_{k|k}^{i,j}$ denotes the target estimation by associating the jth measurement to the ith target, $P_{k|k}^{i,j}$ the corresponding covariance, and $\beta_j^i = p(\theta_k^i = j|\chi_k^i, Z_k)$ the existence-conditioned marginal association probability that the jth measurement is associated with the ith target. Note that the hypothesis-conditioned estimation $(x_{k|k}^{i,j}, P_{k|k}^{i,j})$ can be calculated with a standard Kalman filter algorithm. Notice that if an existing target is miss detected at one scan, its posterior estimation is constrained as its corresponding prediction, that is, $(x_{k|k}^{i,j}, P_{k|k}^{i,j}) = (x_{k|k-1}^i, P_{k|k-1}^i)$, in track update.

According to Bayesian theory, the existence-conditioned marginal association probability $p(\theta_k^i|\chi_k^i, Z_k)$ is determined by

$$p(\theta_k^i|\chi_k^i, Z_k) = \frac{p(\theta_k^i, \chi_k^i|Z_k)}{p(\chi_k^i|Z_k)} = \frac{p(\chi_k^i|\theta_k^i, Z_k)p(\theta_k^i|Z_k)}{p(\chi_k^i|Z_k)} \qquad (8)$$

where the hypothesis-conditioned existence probability $p(\chi_k^i|\theta_k^i, Z_k)$ is determined as

$p(\chi_k^i|\theta_k^i, Z_k)$

$$\propto \begin{cases} \dfrac{p(\chi_k^i|Z_{k-1})(1-P_D)}{1-p(\chi_k^i|Z_{k-1})+p(\chi_k^i|Z_{k-1})(1-P_D)}, & \theta_k^i = 0 \\ 1, & \theta_k^i = j \\ \dfrac{P_D\lambda_B p(z_k^j|x_b)}{\lambda_{FA}+P_D\lambda_B p(z_k^j|x_b)}, & \theta_k^{N_{k-1}+j} = N_{k-1}+j \end{cases}$$

$$\qquad (9)$$

and the posterior existence probability is given by

$$p(\chi_k^i|Z_k) = \sum_{\theta_k^i} p(\theta_k^i, \chi_k^i|Z_k) \qquad (10)$$

with

$$p(\theta_k^i, \chi_k^i|Z_k) = p(\chi_k^i|\theta_k^i, Z_k)p(\theta_k^i|Z_k) \qquad (11)$$

According to the law of total probability, $p(\theta_k^i|Z_k)$ can be theoretically calculated by enumerating all possible joint hypotheses as

$$p(\theta_k^i = j|Z_k) = \sum_{\theta_k^i(\in \Theta_k)=j} p(\Theta_k|Z_k) \qquad (12)$$

where the posterior distribution of the joint association event $p(\Theta_k|Z_k)$ is given by

$$p(\Theta_k|Z_k) \propto \left[\prod_{i\in[N_{k|k-1}],\theta_k^i=0} 1-P_D p(\chi_k^i|Z_{k-1}) \right]$$

$$\times \left[\prod_{i\in[N_{k|k-1}],\theta_k^i=j} P_D p(\chi_k^i|Z_{k-1})p(z_k^j|x_{k|k-1}^i) \right]$$

$$\times \left[\prod_{\theta_k^{N_{k|k-1}+j}=N_{k|k-1}+j} \lambda_{FA} + P_D\lambda_B p(z_k^j|x_b) \right] \qquad (13)$$

where x_b denotes the candidate states of new born targets.

In summary, each track in JPDA is updated through Eqs. (7–12). The outputs of JPDA at each time instant are the posterior existence probability $p(\chi_k^i|Z_k)$ and posterior state estimate $(x_{k|k}^i, P_{k|k}^i)$. Note that the number of targets can be easily estimated by counting the confirmed tracks. Therefore, JPDA provides a complete framework for MTT and track management.

IV. Cost Function Formulation

For UAV trajectory optimization, formulating a pertinent cost function is of paramount importance. JPDA filter provides sequential estimation of the target states as well as the number of targets. Because both target states and number of targets are typically time varying in MTT, the cost function should, therefore, provide an overall evaluation to quantify the performance of both cardinality and state estimations. The optimal subpattern assignment (OSPA) distance, proposed in [33], provides an overall evaluation of cardinality and position estimation performance for MTT. However, calculating this metric requires the knowledge of ground truth, which is obviously not available to the UAV. For this reason, this Note will formulate an alternative cost function, which is defined based on the average expected estimation variances of multitarget state and target number, for UAV trajectory optimization. More specifically, the proposed cost function J is defined as

$$J = \omega J_s + (1-\omega)J_n \qquad (14)$$

where J_s is related to the one-step expected estimation variance of multitarget state; J_n quantifies the one-step expected estimation variance of target number; and $\omega \in [0, 1]$ is a weighting factor. Note that, in order to enforce the balance between multitarget state estimation variance and target number estimation variance in cost function J, both J_s and J_n are normalized to be dimensionless.

The reason behind choosing this cost function is clear: minimizing the estimation variance can increase the confidence of the tracker, thus indirectly improving the estimation accuracy. Obviously, increasing the value of ω enforces more penalty on the performance of multitarget state estimation. It is clear that the cost function J at time instant k is a function of UAV's heading angle $\psi_{u,k}$, and calculating the cost function J requires running JPDA to get the predicted or expected performance. To this end, we manually generate one-step predicted measurement set $\bar{Z}_k$ using currently confirmed targets and available environmental information, that is, P_D, λ_{FA}, and λ_B. These virtual measurements are then used to run JPDA for computing the cost function.

A. Calculation of J_s

In target tracking or localization, the primary interest is to accurately estimate the positions of targets. For this reason, we calculate J_s based on multitarget position estimation variance. From Eq. (6), we know that the original MMSE estimate of the ith target is given by a Gaussian mixture $\sum_{j=0}^{M_k} \beta_j^i \mathcal{N}(\cdot; x_{k|k}^{i,j}, P_{k|k}^{i,j})$ due to the nature of data association uncertainty. Let us define $p_k^{i,j} = [p_{x,k}^{i,j}, p_{y,k}^{i,j}]^T$ as the position estimation vector of the ith target extracted from $x_{k|k}^{i,j}$. Then, the variance of $p_k^{i,j}$ of the ith target can be readily calculated as

$$\text{Var}[p_k^{i,j}] = \begin{bmatrix} E[(p_{x,k}^{i,j} - E[p_{x,k}^{i,j}])^2] & E[(p_{x,k}^{i,j} - E[p_{x,k}^{i,j}])(p_{y,k}^{i,j} - E[p_{y,k}^{i,j}])] \\ E[(p_{y,k}^{i,j} - E[p_{y,k}^{i,j}])(p_{x,k}^{i,j} - E[p_{x,k}^{i,j}])] & E[(p_{y,k}^{i,j} - E[p_{y,k}^{i,j}])^2] \end{bmatrix}$$

$$= \begin{bmatrix} \text{Var}[p_{x,k}^{i,j}] & E[(p_{x,k}^{i,j} - E[p_{x,k}^{i,j}])(p_{y,k}^{i,j} - E[p_{y,k}^{i,j}])] \\ E[(p_{y,k}^{i,j} - E[p_{y,k}^{i,j}])(p_{x,k}^{i,j} - E[p_{x,k}^{i,j}])] & \text{Var}[p_{y,k}^{i,j}] \end{bmatrix}$$

$$\tag{15}$$

where

$$\text{Var}[p_{x,k}^{i,j}] = E[(p_{x,k}^{i,j} - E[p_{x,k}^{i,j}])^2] = E[(p_{x,k}^{i,j})^2] - E[p_{x,k}^{i,j}]^2$$
$$= \sum_{j=0}^{M_k} \beta_j^i (p_{x,k}^{i,j})^2 - \left(\sum_{j=0}^{M_k} \beta_j^i (p_{x,k}^{i,j}) \right)^2 \tag{16}$$

and

$$\text{Var}[p_{y,k}^{i,j}] = \sum_{j=0}^{M_k} \beta_j^i (p_{y,k}^{i,j})^2 - \left(\sum_{j=0}^{M_k} \beta_j^i (p_{y,k}^{i,j}) \right)^2 \tag{17}$$

As it would be beneficial to consider a scalar objective function instead of a matrix form for the trajectory optimization, we leverage the trace of $\text{Var}[p_k^{i,j}]$, denoted as σ_p^i, to quantify the position estimation uncertainty of the ith target as

$$\sigma_p^i = \text{Trace}(\text{Var}[p_k^{i,j}]) = \text{Var}[p_{x,k}^{i,j}] + \text{Var}[p_{y,k}^{i,j}] \tag{18}$$

Note that JPDA approximates the posterior Gaussian mixture $\sum_{j=0}^{M_k} \beta_j^i \mathcal{N}(\cdot; x_{k|k}^{i,j}, P_{k|k}^{i,j})$ by a single Gaussian using moment matching to reduce the computational burden. The approximation error of this simple moment-preserving approach increases with higher modality of the Gaussian mixture. Because the modality of Gaussian mixture $\sum_{j=0}^{M_k} \beta_j^i \mathcal{N}(\cdot; x_{k|k}^{i,j}, P_{k|k}^{i,j})$ can be characterized by the variances of $x_{k|k}^{i,j}$, minimizing $\text{Var}[p_k^{i,j}]$ provides the possibility to improve the quality of data association in JPDA. This is clearly helpful in improving the multitarget state estimation performance. From Eqs. (16) and (17), it is easy to verify that the position estimation variances of the ith target are minimized as $\text{Var}[p_{x,k}^{i,j}] = 0$ and $\text{Var}[p_{y,k}^{i,j}] = 0$ if and only if there exists one j' such that $\beta_{j'}^i = 1$ and $\beta_j^i = 0, \forall j \neq j'$. This obviously coincides with the ideal case with no data association uncertainty. Furthermore, one can also imply that both $\text{Var}[p_{x,k}^{i,j}]$ and $\text{Var}[p_{y,k}^{i,j}]$ take their maximum values once all candidate association pairs of the ith target are equally possible, that is, $\beta_j^i = 1/(M_k + 1)$. This condition corresponds to the largest data association uncertainty and the highest modality of Gaussian mixture $\sum_{j=0}^{M_k} \beta_j^i \mathcal{N}(\cdot; x_{k|k}^{i,j}, P_{k|k}^{i,j})$, in which all Gaussian terms are equally important. The maximum values of $\text{Var}[p_{x,k}^{i,j}]$ and $\text{Var}[p_{y,k}^{i,j}]$ are, respectively, determined as

$$\max\{\text{Var}[p_{x,k}^{i,j}]\} = \frac{M_k}{(M_k + 1)^2} \sum_{j=0}^{M_k} (p_{x,k}^{i,j})^2$$

$$\max\{\text{Var}[p_{y,k}^{i,j}]\} = \frac{M_k}{(M_k + 1)^2} \sum_{j=0}^{M_k} (p_{y,k}^{i,j})^2 \tag{19}$$

For all confirmed tracks, the position estimation variance is normalized to be dimensionless as

$$\sigma_{\bar{p}}^i = \frac{\sigma_p^i}{\max\{\sigma_p^i\}} \tag{20}$$

where the denominator finds the maximum individual variance from all σ_p^i.

Notice that each track has its corresponding existence probability ρ_k^i. Therefore, it is natural to enforce more penalty on the track that has higher existence probability. With this in mind, J_s is defined as a weighted arithmetic mean of $\sigma_{\bar{p}}^i$ as

$$J_s = \frac{\sum_{i=1}^{N_{k|k}} \rho_k^i \sigma_{\bar{p}}^i}{\sum_{i=1}^{N_{k|k}} \rho_k^i} \tag{21}$$

It follows from Eq. (21) that tracks with a high existence probability contribute more to the weighted mean than tracks with a low existence probability. Therefore, minimizing J_s also provides the possibility to improve the quality of track management: discriminating real targets from false alarms.

Remark 2: Although $P_{k|k}^{i,j}$ characterizes the estimation accuracy of the ith target conditioned on the jth measurement, leveraging $\sum_{j=0}^{M_k} \beta_j^i \text{trace}(P_{k|k}^{i,j})$ as the performance measure for the ith target in trajectory optimization is not meaningful for MTT, because there only exists at most one measurement that comes from the ith target in reality. Instead, minimizing σ_p^i, shown in Eq. (18), can reduce the multimodality of Gaussian mixture $\sum_{j=0}^{M_k} \beta_j^i \mathcal{N}(\cdot; x_{k|k}^{i,j}, P_{k|k}^{i,j})$, thus improving data association quality.

B. Calculation of J_n

An MTT algorithm also needs to estimate the number of targets N_k. To this end, J_n will be defined based on the variance of cardinality estimation, which directly indicates the cardinality estimation accuracy. Recall that the outputs of JPDA filter are multitarget state estimates $x_{k|k}^i$ as well as their corresponding existence probabilities ρ_k^i and denote $N_{k|k}^i$ as the cardinality estimate of the ith track. Then, one can easily verify that $N_{k|k}^i$ satisfies a Bernoulli distribution as

$$p(N_{k|k}^i) = \begin{cases} \rho_k^i & \text{if } N_{k|k}^i = 1, \\ 1 - \rho_k^i & \text{if } N_{k|k}^i = 0 \end{cases} \tag{22}$$

From the property of Bernoulli distribution, one can conclude that the expectation and variance of $N_{k|k}^i$ are, respectively, given by

$$E[N_{k|k}^i] = \rho_k^i \tag{23}$$

$$\text{Var}[N_{k|k}^i] = E[(N_{k|k}^i)^2] - E[N_{k|k}^i]^2 \quad = \rho_k^i(1 - \rho_k^i) \tag{24}$$

Notice that, in JPDA filter derivations, the estimations of all tracks are assumed to be independent. Then, according to Bienayme formula, the variance of target number estimation $\text{Var}[N_{k|k}]$ can be readily obtained as

$$\text{Var}[N_{k|k}] = \text{Var}\left[\sum_{i=1}^{N_{k|k}} N_{k|k}^i \right] = \sum_{i=1}^{N_{k|k}} (\text{Var}[N_{k|k}^i])$$

$$= \sum_{i=1}^{N_{k|k}} \rho_k^i(1 - \rho_k^i) \tag{25}$$

Clearly, $\text{Var}[N_{k|k}]$ achieves the minimum value zero at either $\rho_k^i = 1$ or $\rho_k^i = 0$, which corresponds to target always being existence or nonexistence. When $\rho_k^i = 0.5$, $\text{Var}[N_{k|k}]$ takes its maximum value $N_{k|k}/4$. This means that, when the posterior target existence probability equals 0.5, JPDA filter has the least confidence in its cardinality estimation, leading to the increase of cardinality estimation error.

To provide a linear combination of J_s and J_n in cost function J, we define J_n as the normalized version of $\text{Var}[N_{k|k}]$ as

$$J_n = \frac{\sum_{i=1}^{N_{k|k}} \rho_k^i(1 - \rho_k^i)}{\max\{\rho_k^i(1 - \rho_k^i)\}} \tag{26}$$

where the denominator finds the maximum individual variance from all $\text{Var}[N_{k|k}^i]$.

From the aforementioned derivations, we know that the cardinality estimation performance related term J_n depends only on existence probability, whereas the multitarget state estimation performance

---

Algorithm 1:   Trajectory optimization for MTT using JPDA filter at time instant k

---

Input: Current estimation $(x_{k|k}^i, P_{k|k}^i)$, maximum allowable turning rate $\dot{\psi}_{\max}$, number of admissible heading angles L, and previous heading angle $\psi_{u,k-1}$

Output: Optimal UAV heading angle $\psi_{u,k}^*$

1:    $J \leftarrow +\infty$; (initialize the cost function)
2:    $\psi_{\text{low}} \leftarrow \psi_{u,k-1} - \dot{\psi}_{\max} T_s$
3:    $\Delta\psi \leftarrow (2\dot{\psi}_{\max} T_s / L)$
4:    Create the admissible heading angle set Ψ using Eq. (30)
5:    **for** $l = 0, 1, \ldots, L$ **do**
6:        $\psi_{u,\text{temp}} \leftarrow \psi_{\text{low}} + l\Delta\psi$
7:        Calculate the one-step target position prediction using $\psi_{u,\text{temp}}$ and Eq. (1)
8:        Generate virtual measurement set $\bar{Z}_k$
9:    Run JPDA filter using virtual measurements $\bar{Z}_k$
10:        Calculate J_s and J_n as discussed in Sec. IV
11:        $J_{\text{temp}} \leftarrow \omega J_s + (1 - \omega)J_n$
12:        **if** $J_{\text{temp}} < J$ **then**
13:            $J \leftarrow J_{\text{temp}}$
14:            $\psi_{u,k}^* \leftarrow \psi_{u,\text{temp}}$
15:        **end if**
16:    **end for**

---

related term J_s depends on both state estimates and existence probability.

V.   Trajectory Optimization Solution

The aim of the trajectory optimization is to determine UAV's optimal heading angle that minimizes the cost function (14) so as to indirectly increase the estimation performance of JPDA filter. To accomplish this goal, a discrete-time-constrained trajectory optimization problem is formulated, which is denoted as CTO_1. CTO_1: Find

$$\psi_{u,k}^* = \min_{\psi_{u,k}} J(\psi_{u,k}) \tag{27}$$

subject to

$$|\psi_{u,k} - \psi_{u,k-1}| \leq \dot{\psi}_{\max} T_s \tag{28}$$

Constraint (28) corresponds to the physical limit of turning rate, as discussed in Sec. II.A. Note that although the proposed problem considers only one-step-ahead optimization, the optimization problem formulated can be easily extended to a multistep-ahead optimization framework at the sacrifice of computational cost.

Because the objective function described by Eq. (14) is in general nonconvex, the constrained trajectory optimization problem CTO_1 is generally not a convex program. As the operational environment becomes more complicated, for example, the number of targets increases, CTO_1 becomes more complicated to be solved. This implies that finding the exact solution of CTO_1 in a polynomial time is not likely feasible. Therefore, this Note attempts to find an approximate solution of CTO_1 to mitigate the computation issue resulting from the nonconvexity. By approximation, it is expected that the optimal solution of the approximated problem can be obtained in a matter of a few seconds. The approximated constrained trajectory optimization problem, denoted as CTO_2, is: CTO_2: Find

$$\psi_{u,k}^* = \min_{\psi_{u,k} \in \Psi} J(\psi_{u,k}) \tag{29}$$

subject to

$$\Psi = \{\psi_{\text{low}}, \psi_{\text{low}} + \Delta\psi, \psi_{\text{low}} + 2\Delta\psi, \ldots, \psi_{\text{low}} + (L-1)\Delta\psi\} \tag{30}$$

where

$$\psi_{\text{low}} = \psi_{u,k-1} - \dot{\psi}_{\max} T_s \tag{31}$$

$$\Delta\psi = \frac{2\dot{\psi}_{\max} T_s}{L} \tag{32}$$

As can be noticed, CTO_2 is discretized to reduce computational load in finding the solution of the trajectory optimization problem. By defining an admissible heading angle command set Ψ, CTO_2 is set to find the optimal commands from a set of L discretized heading angles. Note that, with the definition of the feasible solution set Ψ, the obtained heading angle command automatically satisfies constraint (28). Note that this approximation strategy is also accepted to relax computational burden in other well-known algorithms such as the methods proposed in [34,35].

The proposed algorithm of trajectory optimization for MTT using JPDA filter is summarized in Algorithm 1.

Remark 3: Because the number of feasible heading angle commands is constrained to be finite, the exact solution of CTO_2 (or the approximate solution of CTO_1) can be easily found through exhaustive search. Therefore, as the size of Ψ increases, the solution of CTO_2 is expected to become closer to the solution of CTO_1 at the expense of increased computational load.

VI.   Numerical Simulations

In this section, the effectiveness of the proposed trajectory optimization algorithm is demonstrated through Monte-Carlo simulations in a cluttered environment. In addition, this section also conducts the performance comparison of the proposed algorithm against nonoptimized trajectories.

A.   Simulation Setup

Our experiments explore a scenario that 1 UAV tracks 10 moving targets with different birth times. The UAV is initially located at $(0 \text{ m}, -3000 \text{ m})$ with heading angle $\psi_{u,1} = 90°$. The velocity of the UAV is $V_u = 40 \text{ m/s}$ and the heading angle is constrained by maximum permissible turning rate $\dot{\psi}_{\max} = 0.1415 \text{ rad/s}$. This corresponds to a maximum bank angle around $30°$. For simplicity, the well-known constant velocity model is used as the transition model $f_k^i(x_k^i)$ as

$$x_k^i = F_k x_k^i + w_{k-1}^i \tag{33}$$

with

$$F_k = \begin{bmatrix} I_2 & T_s I_2 \\ 0_2 & I_2 \end{bmatrix} \tag{34}$$

where the notation 0_2 denotes a 2×2 zero matrix and I_2 stands for a 2×2 identity matrix. The sampling time is given by $T_s = 1$ s. The covariance matrix Q_k of the process noise is defined as [36]
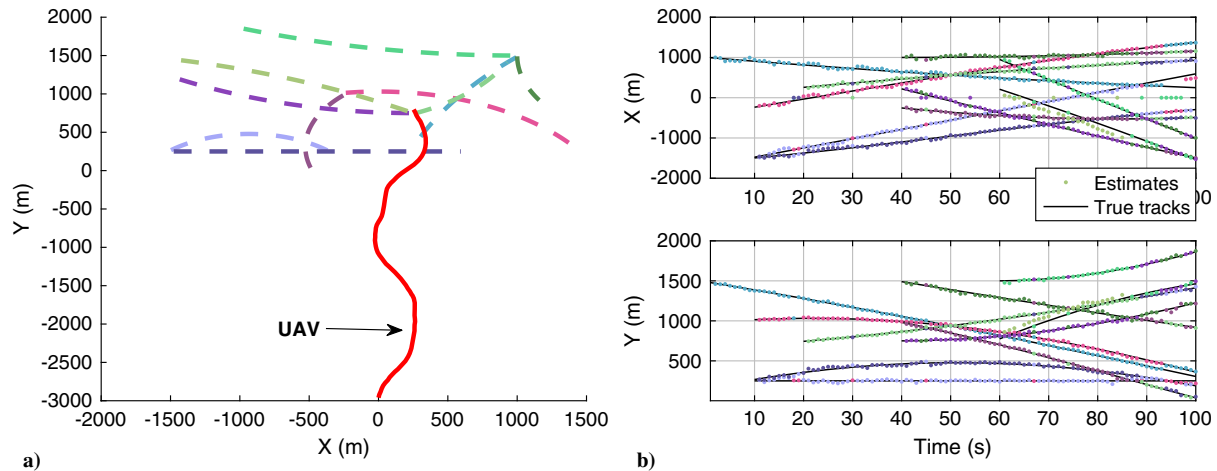
Fig. 1 A snapshot of one sample of the considered scenario. a) Two-dimensional trajectories of the UAV and targets. The dashed color lines are target ground truth trajectories, and the solid red line is the UAV trajectory obtained by the proposed algorithm. b) Time histories of target ground truth trajectories and estimated trajectories.

$$Q_k = \sigma_v^2 \begin{bmatrix} \frac{T_s^4}{4} I_2 & \frac{T_s^3}{2} I_2 \\ \frac{T_s^3}{2} I_2 & T_s^2 I_2 \end{bmatrix} \qquad (35)$$

where the standard deviation of the process noise is given by $\sigma_v = 15$ m/s^2.

The UAV is equipped with an active sensor, which provides range as well as bearing measurements. Therefore, each target-generated measurement z_k^i can be modeled by

$$z_k^i = \begin{bmatrix} \sqrt{(p_{x,k}^i - p_{x,k}^u)^2 + (p_{y,k}^i - p_{y,k}^u)^2} \\ \arctan\left(\frac{p_{y,k}^i - p_{y,k}^u}{p_{x,k}^i - p_{x,k}^u}\right) \end{bmatrix} + v_k \qquad (36)$$

where $v_k \sim \mathcal{N}(\cdot; 0, R_k)$ is the Gaussian measurement noise with $R_k = \text{diag}(\sigma_r^2, \sigma_\theta^2)$, $\sigma_r = 5$ m, and $\sigma_\theta = 1°$. To accommodate the nonlinear measurements, the well-known EKF is used in JPDA filter for measurement update of each target.

The average number of false alarms at each scan is set as $N_{FA} = 20$. Gating is performed with a threshold such that the gating probability is $P_G = 0.999$ to reduce the computation burden of JPDA. The surviving probability for propagating target existence probability is set as $P_S = 0.99$. A tentative track is confirmed if the existence probability satisfies $p(\chi_k^i | Z_k) \geq 0.8$ and a confirmed track is deleted immediately once $p(\chi_k^i | Z_k) \leq 0.1$. The number of Monte-Carlo runs is set as 500 for all tested cases. Figure 1a shows a snapshot of one sample of the considered scenario, where the dashed color lines are target ground truth trajectories, and the solid red line is the UAV trajectory obtained by the proposed algorithm. The time histories of target ground truth trajectories and estimated trajectories are presented in Fig. 1b.

B. Performance Metric

The OSPA distance metric [33] is considered here for overall evaluation of performance, namely, cardinality and position estimation errors. Let X and Y be the position estimation set and true target position set, respectively. The cardinality of these two sets are m and n, respectively. Then, for $c > 0$ and $1 \leq p < \infty$, the OSPA distance $d_p^c(X, Y)$ is given by the combination of the localization and cardinality error as

$$d_p^c(X, Y) \triangleq \begin{cases} \left[\frac{1}{n}\left(\min_{\pi \in \Pi_n} \sum_{i=1}^m d^c(x_i, y_{\pi(i)})^p + c^p(n - m)\right)\right]^{1/p}, & m \leq n \\ d_p^c(Y, X), & m > n \end{cases} \qquad (37)$$

where Π_n denotes the set of all permutations on $\{1, 2, \ldots, n\}$ for any positive integer n. $d^c(x_i, y_{\pi(i)}) = \min(d(x_i, y_{\pi(i)}), c)$ is the cutoff Euclidean distance between two vectors, with $d(x_i, y_{\pi(i)})$ being the Euclidean distance. The order parameter p determines the sensitivity of $d_p^c(X, Y)$ in penalizing estimation outliers, whereas the cutoff parameter c determines the relative weighting of the penalties allocated to cardinality and localization errors. In all simulations, these two parameters are set as $p = 1, c = 100$. It should be pointed out that the OSPA distance reduces to the summation of localization and cardinality estimation errors by choosing $p = 1$. With this in mind, it is expected that the proposed cost function (14) with $\omega = 0.5$ would provide the best solution in terms of OSPA performance.

For the purpose of analyzing the characteristics of the proposed algorithm, the localization and cardinality errors are also used as performance metrics in the simulations. These two performance metrics are defined as

$$d_{p,\text{loc}}^c(X, Y) \triangleq \begin{cases} \left[\frac{1}{n}\left(\min_{\pi \in \Pi_n} \sum_{i=1}^m d^c(x_i, y_{\pi(i)})^p\right)\right]^{1/p}, & m \leq n \\ d_{p,\text{loc}}^c(Y, X), & m > n \end{cases} \qquad (38)$$

$$d_{p,\text{card}}^c(X, Y) \triangleq \begin{cases} \left[\frac{1}{n}(c^p(n - m))\right]^{1/p}, & m \leq n \\ d_{p,\text{card}}^c(Y, X), & m > n \end{cases} \qquad (39)$$

As expected, increasing the weighting factor ω in cost function (14) will reduce the localisation error $d_{p,\text{loc}}^c(X, Y)$ because more penalty is enforced on the performance of target state estimation. Similarly, the cardinality error $d_{p,\text{card}}^c(X, Y)$ can be reduced by decreasing the weight factor ω in cost function (14).

C. Characteristics of Proposed Approach

This subsection empirically analyzes the characteristics of the proposed algorithm. For simplicity, we assume that each target is detected with constant detection probability $P_D = 0.9$ in this subsection. We first investigate the characteristics of the proposed algorithm with different weighting factor ω. The Monte-Carlo simulation results of mean OSPA distance with respect to different weighting factors $\omega = 0.2, 0.5, 0.8$ are presented Fig. 2a. The number of admissible heading angle commands at each time instant is set as $L = 10$ in these simulation studies. As expected, increasing the weighting factor ω in cost function (14) will reduce the localization error $d_{p,\text{loc}}^c(X, Y)$ because more penalty is enforced on the performance of target state estimation. Similarly, the cardinality error $d_{p,\text{card}}^c(X, Y)$ can be reduced by decreasing the weight factor ω in cost function (14). Note that the peaks in this figure are resulted from track initialization for new birth targets. The mean value and standard

Table 1 Comparison results of Monte-Carlo simulations with respect to different ω

Scenario		OSPA distance, m	Localization error, m	Cardinality error, m
$\omega = 0.2$	Mean	31.9579	26.9209	5.0370
	Std	9.5639	4.8196	12.9582
$\omega = 0.5$	Mean	24.0348	18.0204	6.0144
	Std	11.7160	5.4368	12.9318
$\omega = 0.8$	Mean	24.0516	17.9289	6.1228
	Std	11.7478	5.6255	12.9264

Table 2 Comparison results of Monte-Carlo simulations with respect to different L

Scenario		OSPA distance, m	Localization error, m	Cardinality error, m
$L = 5$	Mean	24.0012	18.0218	6.1594
	Std	11.8151	5.3620	12.9736
$L = 10$	Mean	23.9663	17.9757	6.0255
	Std	11.8473	5.1969	12.9813
$L = 15$	Mean	23.7745	17.6151	5.9444
	Std	11.8734	5.1950	12.9847

deviation (Std) of OSPA distance, localization error, and cardinality error obtained from Monte-Carlo simulations are summarized in Table 1. From Fig. 2a, it can be noted that, when $\omega < 0.5$, increasing the weighting constant generates significantly improved estimation performance in terms of OSPA distance. When the weighting factor ω exceeds 0.5, the OSPA distance does not show much difference with the variation of ω. This fact can be attributed to the fact that JPDA filter is more sensitive to localization error than cardinality error in the considered scenario, as shown in Table 1. Also, one can observe that the proposed trajectory optimization algorithm with $\omega = 0.5$ provides the best overall performance in terms of OSPA distance. The reason is that the OSPA distance reduces to the summation of localization and cardinality estimation errors with $p = 1$. Clearly, increasing the value of ω provides more accurate estimation of multitarget state, as shown in Table 1, because the proposed cost

function gives more penalty on J_s. Similarly, cardinality estimation performance can be improved with smaller ω. Therefore, the weighting factor ω provides the flexibility to balance between localization error and cardinality error.

As the proposed algorithm finds an approximate solution to the original problem by control input discretization, the size of the set of admissible heading angle commands, for example, L, plays an important role in governing the performance of the proposed algorithm. For this reason, comparison simulations with different $L = 5, 10, 15$ are carried out to analyze the sensitivity of the proposed approach against L. The weighting factor ω is set as $\omega = 0.5$ in the simulations. The Monte-Carlo simulation results of mean OSPA distance are presented in Fig. 2b. The mean value and standard deviation (Std) of OSPA distance, localization error, and cardinality error obtained from Monte-Carlo simulations are summarized in Table 2. Unsurprisingly, increasing the value of L generates improved
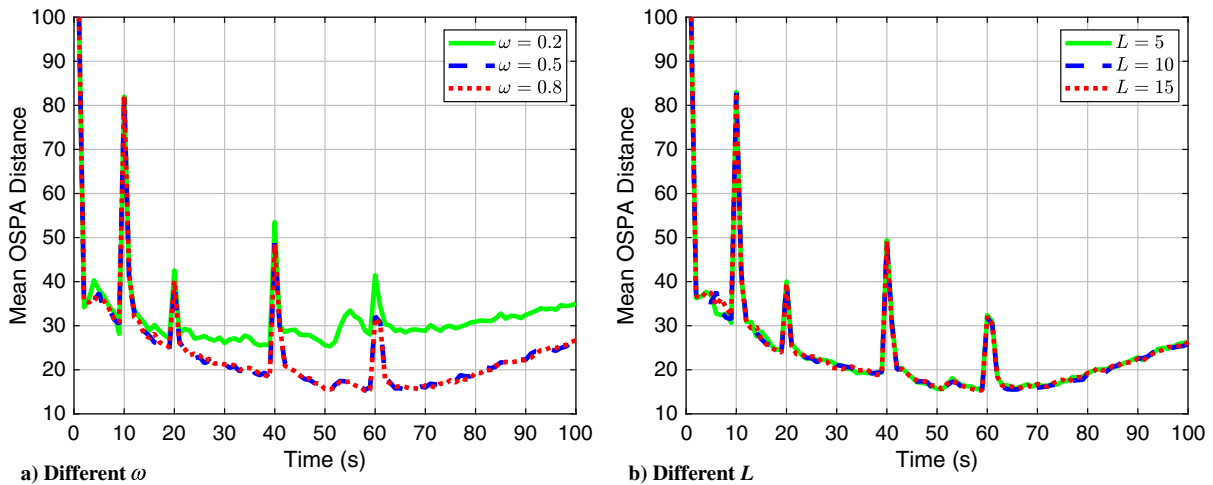

a) Different ω b) Different L

Fig. 2 Mean OSPA distance comparisons.
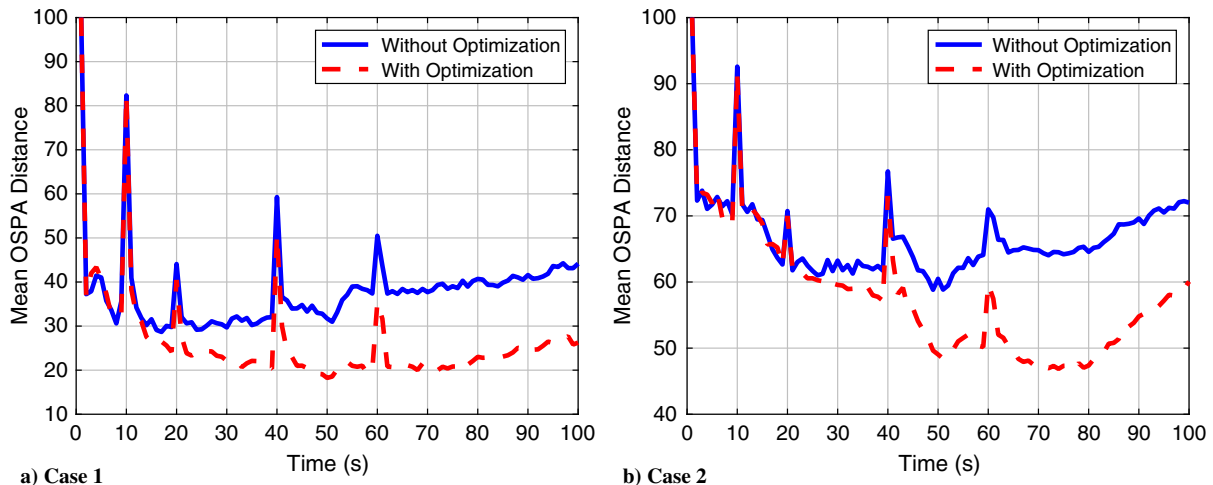

a) Case 1   b) Case 2

Fig. 3 Mean OSPA distance comparisons.

results as the approximated optimization problem CTO_2 is closer to the original problem CTO_1, as discussed in Sec. V. However, this benefit, in return, requires higher computational cost, which might not be available for small-scale UAVs. From Fig. 2b, it can be easily concluded that the estimation performance under the proposed algorithm does not differ much with different values of L. This fact confirms that the proposed algorithm is robust against the variation of L.

D. Comparison with Nonoptimized Trajectory

To further show the effectiveness of the proposed trajectory optimization algorithm, we compare the optimized trajectories with trajectories without optimization for two different cases: 1) constant detection probability $P_D = 0.9$; 2) time-varying detection probability $P_D = 0.9e^{-r_k^i/6000}$. The weighting factor ω is set as $\omega = 0.5$, and the discretization size is selected as $L = 10$ in the comparison studies. For trajectories without optimization, we randomly pick one admissible heading angle command from Ψ at every time instant. The comparison results of mean OSPA distance for cases 1 and 2 obtained from Monte-Carlo simulations are provided in Figs. 3a and 3b, respectively. From these two figures, one can note that the optimized UAV trajectory significantly improves the overall estimation performance in both cases. When the detection probability P_D is high (i.e., case 1), the improvement in performance almost starts at the initial point and an approximate 25% improvement in steady-state estimation accuracy has been achieved. For case 2, because the initial detection probability is very low, below 0.5, the optimized trajectory does not show much performance improvement over nonoptimized trajectory. However, as the proposed algorithm guides the UAV toward the targets, as shown in Fig. 1, the detection probability P_D gradually increases. Therefore, the optimized trajectory generated leads to significant improvements in estimation performance after a certain period, as can be confirmed from Fig. 3b. Compared with the nonoptimized trajectory, we can also note from this figure that the proposed algorithm brings around 15% improvement in the steady-state localization accuracy for case 2.

VII.   Conclusions

A constrained trajectory optimization algorithm has been proposed for a fixed-wing UAV to improve target localization accuracy in tracking multiple moving targets. The UAV is assumed to use the JPDA filter as the baseline multitarget tracker. A cost function is first formulated based on the variance of multitarget state estimation and the variance of cardinality estimation. Because the cost function developed quantifies the confidence of the tracker, improved estimation performance can be obtained by minimizing the cost function. To approximate the practical situations at most, the physical control limit is also considered in the proposed optimization problem. The original nonconvex optimization problem is relaxed by discretizing the admissible set of heading commands, and the suboptimal heading angle is then obtained by exhaustive search. Extensive numerical simulations clearly validate the effectiveness of the proposed algorithm and demonstrate that the algorithm developed brings significant performance improvement, compared with nonoptimized trajectory. Future study will consider extending the proposed algorithm to multi-UAV MTT scenarios.

References

[1] Delande, E., Frueh, C., Franco, J., Houssineau, J., and Clark, D., "Novel Multi-Object Filtering Approach for Space Situational Awareness," *Journal of Guidance, Control, and Dynamics*, Vol. 41, No. 1, 2018, pp. 59–73.
https://doi.org/10.2514/1.G002067

[2] Pak, A., Correa, J., and Adams, M., "Robust Joint Target Detection and Tracking for Space Situational Awareness," *Journal of Guidance, Control, and Dynamics*, Vol. 41, No. 1, 2018, pp. 119–136.
https://doi.org/10.2514/1.G002231

[3] Oh, H., Shin, H.-S., Kim, S., and Chen, W.-H., "Communication-Aware Trajectory Planning for Unmanned Aerial Vehicles in Urban Environments," *Journal of Guidance, Control, and Dynamics*, Vol. 41,

No. 10, 2018, pp. 2271–2282.
https://doi.org/10.2514/1.G003099

[4] Oh, H., Kim, S., Shin, H.-S., and Tsourdos, A., "Coordinated Standoff Tracking of Moving Target Groups Using Multiple UAVs," *IEEE Transactions on Aerospace and Electronic Systems*, Vol. 51, No. 2, 2015, pp. 1501–1514.
https://doi.org/10.1109/TAES.2015.140044

[5] Ding, R., Yu, M., Oh, H., and Chen, W.-H., "New Multiple-Target Tracking Strategy Using Domain Knowledge and Optimization," *IEEE Transactions on Systems, Man, and Cybernetics: Systems*, Vol. 47, No. 4, 2017, pp. 605–616.
https://doi.org/10.1109/TSMC.6221021

[6] Ibrahim, A. W. N., Ching, P. W., Seet, G. G., Lau, W. M., and Czajewski, W., "Moving Objects Detection and Tracking Framework for UAV-Based Surveillance," *2010 4th Pacific-Rim Symposium on Image and Video Technology (PSIVT)*, IEEE, New York, 2010, pp. 456–461.
https://doi.org/10.1109/PSIVT.2010.83

[7] Hwang, I., Balakrishnan, H., Roy, K., and Tomlin, C., "Multiple-Target Tracking and Identity Management with Application to Aircraft Tracking," *Journal of Guidance, Control, and Dynamics*, Vol. 30, No. 3, 2007, pp. 641–653.
https://doi.org/10.2514/1.27366

[8] Singer, R., Sea, R., and Housewright, K., "Derivation and Evaluation of Improved Tracking Filter for Use in Dense Multitarget Environments," *IEEE Transactions on Information Theory*, Vol. 20, No. 4, 1974, pp. 423–432.
https://doi.org/10.1109/TIT.1974.1055256

[9] Musicki, D., Evans, R., and Stankovic, S., "Integrated Probabilistic Data Association," *IEEE Transactions on Automatic Control*, Vol. 39, No. 6, 1994, pp. 1237–1241.
https://doi.org/10.1109/9.293185

[10] Fortmann, T., Bar-Shalom, Y., and Scheffe, M., "Sonar Tracking of Multiple Targets Using Joint Probabilistic Data Association," *IEEE Journal of Oceanic Engineering*, Vol. 8, No. 3, 1983, pp. 173–184.
https://doi.org/10.1109/JOE.1983.1145560

[11] Stauch, J., Bessell, T., Rutten, M., Baldwin, J., Jah, M., and Hill, K., "Joint Probabilistic Data Association and Smoothing Applied to Multiple Space Object Tracking," *Journal of Guidance, Control, and Dynamics*, Vol. 41, No. 1, 2018, pp. 19–33.
https://doi.org/10.2514/1.G002230

[12] Reid, D., "An Algorithm for Tracking Multiple Targets," *IEEE Transactions on Automatic Control*, Vol. 24, No. 6, 1979, pp. 843–854.
https://doi.org/10.1109/TAC.1979.1102177

[13] Cox, I. J., and Hingorani, S. L., "An Efficient Implementation of Reid's Multiple Hypothesis Tracking Algorithm and Its Evaluation for the Purpose of Visual Tracking," *IEEE Transactions on Pattern Analysis and Machine Intelligence*, Vol. 18, No. 2, 1996, pp. 138–150.
https://doi.org/10.1109/34.481539

[14] He, S., Shin, H.-S., and Tsourdos, A., "Track-Oriented Multiple Hypothesis Tracking Based on Tabu Search and Gibbs Sampling," *IEEE Sensors Journal*, Vol. 18, No. 1, 2017, pp. 328–339.
https://doi.org/10.1109/JSEN.2017.2758846

[15] Hodgson, J., "Trajectory Optimization Using Differential Inclusion to Minimize Uncertainty in Target Location Estimation," *AIAA Guidance, Navigation, and Control Conference and Exhibit*, AIAA Paper 2005-6187, 2005.
https://doi.org/10.2514/6.2005-6187

[16] Narkiewicz, J. P., Kopyt, A., Radyisyewski, P., and Malecki, T., "Optimal Selection of UAV for Ground Target Tracking," *AIAA Modeling and Simulation Technologies Conference*, AIAA Paper 2015-2330, 2015.
https://doi.org/10.2514/6.2015-2330

[17] He, S., Shin, H.-S., and Tsourdos, A., "Trajectory Optimization for Target Localization with Bearing-Only Measurement," *IEEE Transactions on Robotics*, Vol. 35, No. 3, 2019, pp. 653–668.
https://doi.org/10.1109/TRO.8860

[18] Le Cadre, J., "Optimization of the Observer Motion for Bearings-Only Target Motion Analysis," *Proceedings of the 36th IEEE Conference on Decision and Control, 1997*, IEEE, New York, Vol. 4, 1997, pp. 3126–3131.
https://doi.org/10.1109/ADFS.1996.581105

[19] Passerieux, J.-M., and Van Cappel, D., "Optimal Observer Maneuver for Bearings-Only Tracking," *IEEE Transactions on Aerospace and Electronic Systems*, Vol. 34, No. 3, 1998, pp. 777–788.
https://doi.org/10.1109/7.705885

[20] Oshman, Y., and Davidson, P., "Optimization of Observer Trajectories for Bearings-Only Target Localization," *IEEE Transactions on Aerospace and Electronic Systems*, Vol. 35, No. 3, 1999, pp. 892–902.
https://doi.org/10.1109/7.784059

[21] Fosbury, A. M., and Crassidis, J. L., "Optimal Trajectory Determination for Increased Relative Navigation Observability of Air Vehicles," *AIAA Guidance, Navigation, and Control Conference*, AIAA Paper 2008-6648, 2008.
https://doi.org/10.2514/6.2008-6648

[22] Roh, H., Cho, M.-H., and Tahk, M.-J., "Trajectory Optimization Using Cramér-Rao Lower Bound for Bearings-Only Target Tracking," *2018 AIAA Guidance, Navigation, and Control Conference*, AIAA Paper 2018-1591, 2018.
https://doi.org/10.2514/6.2018-1591

[23] Anjaly, P., and Ratnoo, A., "Observability Enhancement of Maneuvering Target with Bearings-Only Information," *Journal of Guidance, Control, and Dynamics*, Vol. 41, No. 1, 2018, pp. 184–198.
https://doi.org/10.2514/1.G003003

[24] Grzymisch, J., and Fichter, W., "Analytic Optimal Observability Maneuvers for In-Orbit Bearings-Only Rendezvous," *Journal of Guidance, Control, and Dynamics*, Vol. 37, No. 5, 2014, pp. 1658–1664.
https://doi.org/10.2514/1.G000612

[25] Grzymisch, J., and Fichter, W., "Optimal Rendezvous Guidance with Enhanced Bearings-Only Observability," *Journal of Guidance, Control, and Dynamics*, Vol. 38, No. 6, 2015, pp. 1131–1140.
https://doi.org/10.2514/1.G000822

[26] Woffinden, D. C., and Geller, D. K., "Optimal Orbital Rendezvous Maneuvering for Angles-Only Navigation," *Journal of Guidance, Control, and Dynamics*, Vol. 32, No. 4, 2009, pp. 1382–1387.
https://doi.org/10.2514/1.45006

[27] Zhou, K., and Roumeliotis, S. I., "Optimal Motion Strategies for Range-Only Constrained Multisensor Target Tracking," *IEEE Transactions on Robotics*, Vol. 24, No. 5, 2008, pp. 1168–1185.
https://doi.org/10.1109/TRO.2008.2004488

[28] Zhou, K., and Roumeliotis, S. I., "Multirobot Active Target Tracking with Combinations of Relative Observations," *IEEE Transactions on Robotics*, Vol. 27, No. 4, 2011, pp. 678–695.
https://doi.org/10.1109/TRO.2011.2114734

[29] Ragi, S., and Chong, E. K., "UAV Path Planning in a Dynamic Environment via Partially Observable Markov Decision Process," *IEEE Transactions on Aerospace and Electronic Systems*, Vol. 49, No. 4, 2013, pp. 2397–2412.
https://doi.org/10.1109/TAES.2013.6621824

[30] Farmani, N., Sun, L., and Pack, D. J., "A Scalable Multitarget Tracking System for Cooperative Unmanned Aerial Vehicles," *IEEE Transactions on Aerospace and Electronic Systems*, Vol. 53, No. 4, 2017, pp. 1947–1961.
https://doi.org/10.1109/TAES.2017.2677746

[31] Hanselmann, T., Morelande, M., Moran, B., and Sarunic, P., "Sensor Scheduling for Multiple Target Tracking and Detection Using Passive Measurements," *2008 11th International Conference on Information Fusion*, IEEE, New York, 2008, pp. 1–8.

[32] Hue, C., Le Cadre, J.-P., and Perez, P., "Posterior Cramer-Rao Bounds for Multi-Target Tracking," *IEEE Transactions on Aerospace and Electronic Systems*, Vol. 42, No. 1, 2006, pp. 37–49.
https://doi.org/10.1109/TAES.2006.1603404

[33] Schuhmacher, D., Vo, B.-T., and Vo, B.-N., "A Consistent Metric for Performance Evaluation of Multi-Object Filters," *IEEE Transactions on Signal Processing*, Vol. 56, No. 8, 2008, pp. 3447–3457.
https://doi.org/10.1109/TSP.2008.920469

[34] Cook, K., Bryan, E., Yu, H., Bai, H., Seppi, K., and Beard, R., "Intelligent Cooperative Control for Urban Tracking," *Journal of Intelligent & Robotic Systems*, Vol. 74, Nos. 1–2, 2014, pp. 251–267.
https://doi.org/10.1007/s10846-013-9896-5

[35] Shin, H.-S., Garcia, A. J., and Alvarez, S., "Information-Driven Persistent Sensing of a Non-Cooperative Mobile Target Using UAVs," *Journal of Intelligent & Robotic Systems*, Vol. 92, Nos. 3–4, 2018, pp. 629–643.
https://doi.org/10.1007/s10846-017-0719-y

[36] Hong, L., "Discrete Constant-Velocity-Equivalent Multirate Models for Target Tracking," *Mathematical and Computer Modelling*, Vol. 28, No. 11, 1998, pp. 7–18.
https://doi.org/10.1016/S0895-7177(98)00161-7